Electron paramagnetic resonance and optical absorption study of V^{4+} centres in YVO_4 crystals

2004 J. Phys.: Condens. Matter 16 7095

(http://iopscience.iop.org/0953-8984/16/39/040)

INSTITUTE OF PHYSICS PUBLISHING JOURNAL OF PHYSICS: CONDENSED MATTER

J. Phys.: Condens. Matter **16** (2004) 7095–7106 PII: S0953-8984(04)82819-4

Electron paramagnetic resonance and optical absorption study of V^{4+} centres in YVO_4 crystals

N Y Garces[1], K T Stevens[2], G K Foundos[2] and L E Halliburton[1,3]

[1] Department of Physics, West Virginia University, Morgantown, WV 26506, USA
[2] Northrop Grumman Space Technology, Synoptics, Charlotte, NC 28273, USA

E-mail: Larry.Halliburton@mail.wvu.edu

Received 29 June 2004
Published 17 September 2004
Online at stacks.iop.org/JPhysCM/16/7095
doi:10.1088/0953-8984/16/39/040

Abstract

Electron paramagnetic resonance (EPR) has been used to characterize three distinct V^{4+} centres in undoped Czochralski-grown yttrium orthovanadate (YVO_4) crystals. These EPR signals are observed at low temperatures, and their average *c*-axis splittings between adjacent ^{51}V hyperfine lines are 40 G, 123 G, and 140 G. We refer to these centres as $[V^{4+}]_A$, $[V^{4+}]_B$, and $[V^{4+}]_C$, respectively. The $[V^{4+}]_A$ and $[V^{4+}]_B$ centres are present in as-grown crystals. Exposure at 77 K to ionizing radiation (x-rays or an ultraviolet laser beam) destroys these centres and creates the $[V^{4+}]_C$ centres. The as-grown state of the crystal is restored upon returning to room temperature. Angular dependence data are used to determine the principal values and principal directions of the **g** tensor and the ^{51}V hyperfine tensor for each of the centres. We suggest that the $[V^{4+}]_A$ centre is a V^{4+} ion adjacent to an oxygen vacancy and that the $[V^{4+}]_B$ centre is a V^{4+} ion substituting for a Y^{3+} ion (i.e. a vanadium antisite defect). The $[V^{4+}]_C$ centre is assigned to a V^{4+} ion at a regular vanadium site with a nearby stabilizing defect, possibly a Zr^{4+} on a Y^{3+} site. In as-grown crystals, there is a correlation between the number of $[V^{4+}]_A$ centres and the intensity (at 380 nm) of a broad near-edge optical absorption band. This band, now associated with oxygen vacancies, gives YVO_4 a 'yellow' appearance.

1. Introduction

Single crystals of yttrium orthovanadate (YVO_4) have useful optical properties in the visible and near-infrared regions of the spectrum and, equally important, they can be grown in large sizes [1, 2]. A significant birefringence [3–6] makes undoped crystals viable candidates for device applications [7–9] in optical telecommunication networks, while neodymium-doped crystals

[3] Author to whom all correspondence should be addressed.

are being widely used as solid-state lasers [10–15]. Planar waveguides have also been produced in YVO_4 crystals by ion implantation with Si^+ ions [16]. At the present time, however, little is known about the point defects in YVO_4 that adversely affect device performance. Although the optical quality of many of the YVO_4 crystals being grown today is very good, some growth runs still result in crystals that have uniformity and colouration problems. Thus, it is important to understand the general defect behaviour of YVO_4 and to identify those specific defects that are responsible for degrading the quality of the material.

Electron paramagnetic resonance (EPR) is a high-resolution technique often used to identify point defects in insulators and semiconductors [17]. In YVO_4, a primary application of EPR has been to characterize rare-earth impurity ions that substitute for yttrium [18–21]. Recently, this technique has been extended to include studies of electron and hole traps in YVO_4 that may be associated with the broad optical absorption bands responsible for the unwanted colour in some of the crystals. Garces *et al* [22] have shown that a silicon impurity (replacing a vanadium ion) will trap a hole on one of its four adjacent oxygen ions when the crystal is exposed to ionizing radiation at 77 K. These are the dominant hole traps in YVO_4. Trapped electron centres, in the form of V^{4+} ions, have also been reported. The presence of a V^{4+} centre in as-grown YVO_4 was first demonstrated by Jablonski *et al* [23] and later verified by Garces *et al* [22]. This centre has an average hyperfine splitting of 123 G when the magnetic field is along the [001] direction (we now refer to it as the $[V^{4+}]_B$ centre). A second V^{4+} centre, formed in YVO_4 during a low-temperature irradiation with x-rays, was reported by Garces *et al* [22]. This latter centre has an average hyperfine splitting of 140 G when the magnetic field is along the [001] direction (we now refer to it as the $[V^{4+}]_C$ centre). In the earlier papers [22, 23], the angular dependence of these two V^{4+} centres were not investigated and specific models were not proposed.

In the present paper, we provide a more complete characterization of the $[V^{4+}]_B$ and the $[V^{4+}]_C$ EPR spectra that were previously observed [22, 23] in YVO_4. We also observe and characterize a third V^{4+} EPR spectrum, not reported until now, that is present in many of the as-grown YVO_4 crystals. This third V^{4+} centre has an average hyperfine splitting of 40 G when the magnetic field is along the [001] direction, and we refer to it as the $[V^{4+}]_A$ centre. The $[V^{4+}]_A$ centre is especially important because we find that its concentration correlates with the unwanted optical absorption occurring near the band edge in some YVO_4 crystals (when present, this band makes the crystals appear yellow). Ionizing radiation (x-rays or 351–364 nm laser light) at 77 K easily produces the $[V^{4+}]_C$ centre and destroys nearly all of the $[V^{4+}]_A$ and the $[V^{4+}]_B$ centres. From the angular variation of each EPR spectrum, we determine the number of equivalent sites, the **g** tensor, and the vanadium hyperfine tensor. Based on these spin-Hamiltonian results and the observed production and decay properties, we propose specific models for the three V^{4+} centres.

2. Experimental procedure

The crystal structure of YVO_4 is tetragonal (space group $I4_1/amd$) with $a = 7.1183$ Å and $c = 6.2893$ Å [24]. It basically consists of $(VO_4)^{3-}$ tetrahedral units and Y^{3+} ions arranged in an alternating sequence along the [001] direction (i.e. the *c*-axis). Each vanadium ion has four equivalent oxygen neighbours arranged in a slightly irregular tetrahedron (elongated along the [001] direction) and each yttrium ion has eight oxygen neighbours (four with one yttrium–oxygen bond length and the other four with a slightly different yttrium–oxygen bond length). The $(VO_4)^{3-}$ units occupy two equivalent sites, related to each other by a 90° rotation about the [001] axis. There are also two Y^{3+} sites related by a 90° rotation about [001].

A set of 14 YVO_4 samples, representing a wide range of defect-related yellow coloration, was used in the present investigation. These undoped single crystals were grown by the Czochralski technique at Northrop Grumman Space Technology (Synoptics) in Charlotte, NC. During growth, the melt was contained in an iridium crucible under an inert atmosphere. The dimensions of our samples were approximately $8.2\times3\times3\,mm^3$, with the 8.2 mm side parallel to the [100] direction (i.e. an *a*-axis). Optical absorption and *c*-axis EPR data from all 14 samples were acquired first, then a smaller sample ($3\times3\times3\,mm^3$) was cut from one of the larger samples and used to obtain the EPR angular dependence data.

The EPR data were taken with a Bruker ESP 300 spectrometer operating near 9.45 GHz. An Oxford Instruments ESR-900 helium-gas-flow system was used to control the temperature, and a proton gaussmeter was used to measure the magnetic field. A MgO:Cr crystal was used to correct the angular dependence data for the small difference in magnetic field between the YVO_4 sample and the gaussmeter probe (the isotropic g value for Cr^{3+} in MgO is 1.9800). Optical absorption data were taken at room temperature with a Perkin–Elmer Lambda 900 spectrophotometer. The known sensitivity of the EPR spectrometer was used to make estimates of defect concentrations (approximately 5×10^{10} spins give a signal-to-noise ratio of 1 at 10 K for a nonsaturating $S = 1/2$ paramagnetic centre having a 1 G linewidth). This procedure is similar to the use of a calibrated standard sample, except we calibrate the spectrometer once using a Bruker weak pitch sample and then check for changes in sensitivity every few months. In our case, all of the EPR spectra used to estimate defect concentrations were taken at the microwave power used in the calibration process. Different measurement temperatures are accounted for by including a T^{-1} factor. Our approach gives error limits of approximately 20% on relative concentrations and a factor of 2 on absolute concentrations.

Two sources of ionizing radiation were used to change the concentrations of the paramagnetic defects (i.e. to change their charge states). The most efficient source was an x-ray tube operating at 60 kV and 30 mA. A less efficient, but still viable, source of ionizing radiation was the multi-line ultraviolet output (351–364 nm) from a cw argon-ion laser. At low temperature, the band edge of YVO_4 shifts to 335 nm and the ultraviolet photons from the laser are not as effective as the x-rays in producing electron-hole pairs (i.e. these ultraviolet photons are absorbed only in the tail of the band edge).

3. Electron paramagnetic resonance results

The EPR spectra of V^{4+} ions ($3d^1$) consist of sets of eight equally intense lines due to resolved hyperfine interactions with the ^{51}V nucleus ($I = 7/2$, 99.75% abundant). These are $S = 1/2$ centres. Two of our V^{4+} spectra, the $[V^{4+}]_A$ centre and the $[V^{4+}]_B$ centre, are present in as-grown YVO_4 crystals. During a 77 K irradiation with x-rays or an ultraviolet laser beam, the $[V^{4+}]_A$ and the $[V^{4+}]_B$ centres decrease significantly and the $[V^{4+}]_C$ centre appears. Warming the irradiated sample to room temperature restores the as-grown state. In this section, the experimental EPR results are separately described for each of the three centres.

3.1. $[V^{4+}]_A$ centre (in as-grown crystals)

The EPR signal referred to as the $[V^{4+}]_A$ centre is shown in figure 1. This spectrum is present, at varying levels of intensity, in many as-grown YVO_4 crystals. The data in figure 1 were obtained at 10 K with the magnetic field parallel to the [001] direction and a 9.443 GHz microwave frequency. This centre does not easily saturate with microwave power and thus is best observed at very low temperatures. We estimate that the concentration of defects represented by the $[V^{4+}]_A$ spectrum in figure 1 is approximately $4\times10^{17}\,cm^{-3}$. The widths of

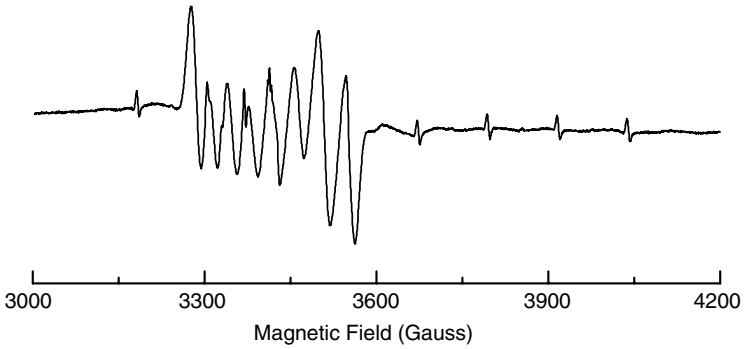

Figure 1. EPR spectrum of the $[V^{4+}]_A$ centre in YVO_4, taken at 10 K with the magnetic field along the [001] direction. The weak, and more widely split, set of eight lines are due to the 'saturated' $[V^{4+}]_B$ centre (see figure 3).

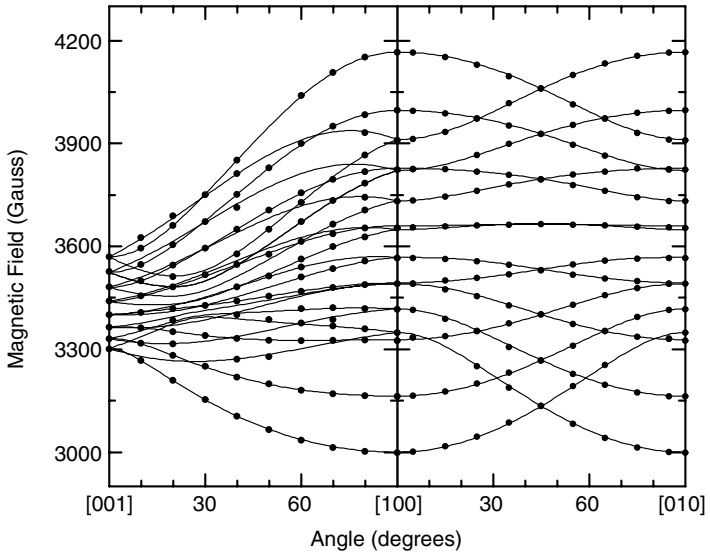

Figure 2. Angular dependence of the $[V^{4+}]_A$ centre for rotations in the (010) and (001) planes. The experimental results, obtained at 10 K, are represented by the discrete data points, while the solid lines were calculated using the **g** and **A** tensors in table 1.

the $[V^{4+}]_A$ centre EPR lines at 10 K are approximately 17 G, which is larger than the widths of 2.9 and 1.6 G found at 30 and 15 K, respectively, for the $[V^{4+}]_B$ and $[V^{4+}]_C$ centres. When comparing the relative concentrations of the $[V^{4+}]_A$ and $[V^{4+}]_B$ centres in as-grown crystals, it is important to take into account the different linewidths and the different temperatures for optimum viewing.

The EPR angular dependence of the $[V^{4+}]_A$ spectrum has been investigated in detail. Data were taken at 10° intervals during rotations in the (010) plane and the (001) plane, and at 15° intervals during rotations in the $(\bar{1}10)$ plane. Results from the (010) and (001) planes are shown in figure 2. For an arbitrary direction of magnetic field, there are four magnetically inequivalent, but crystallographically equivalent, orientations of the defect responsible for the $[V^{4+}]_A$ spectrum. All four sites occupied by this defect are degenerate when the magnetic field

Table 1. Summary of the principal values and principal axis directions for the **g** tensors and ^{51}V hyperfine tensors associated with the three V^{4+} centres in YVO_4. The principal-axis directions correspond to one symmetry-related site for each defect. Estimates of the error limits are ± 0.0005 for the **g** values, ± 3 MHz for the A values, and $\pm 2^\circ$ for the θ and ϕ angles.

		Principal values	Principal axes	
			θ (deg)	ϕ (deg)
$[V^{4+}]_A$ centre				
g	g_1	1.9667	8	0
	g_2	1.8912	90	90
	g_3	1.8610	82	180
A (^{51}V)	A_1	48 MHz	25	0
	A_2	229 MHz	65	180
	A_3	441 MHz	90	90
$[V^{4+}]_B$ centre				
g	g_1	1.9876	102	56
	g_2	1.9235	79	143
	g_3	1.8604	16	15
A (^{51}V)	A_1	45 MHz	76	239
	A_2	98 MHz	92	328
	A_3	332 MHz	14	49
$[V^{4+}]_C$ centre				
g	g_1	1.9642	76	0
	g_2	1.8701	90	90
	g_3	1.7380	14	180
A (^{51}V)	A_1	63 MHz	86	0
	A_2	128 MHz	90	90
	A_3	343 MHz	4	180

is along the [001] or the [110] directions, and the EPR spectrum then consists of a single set of eight lines. The four sites are pairwise degenerate if the magnetic field is rotated in the (001) plane from [100] to [010] or in the $(\bar{1}10)$ plane from [001] to [110] and, in each case, two sets of eight lines are observed. When the magnetic field is rotated in the (010) plane from [001] to [100], two of the sites are degenerate and the other two sites are each nondegenerate, thus giving three sets of eight lines in the EPR spectrum with one set twice as intense as the other two sets.

The following spin-Hamiltonian was used to analyse the angular dependence data obtained from the $[V^{4+}]_A$ centre. It contains the usual Zeeman and hyperfine terms:

$$\mathbf{H} = \beta \mathbf{S}\cdot\mathbf{g}\cdot\mathbf{B} + \mathbf{I}\cdot\mathbf{A}\cdot\mathbf{S} - g_N\beta_N\mathbf{I}\cdot\mathbf{B}. \tag{1}$$

A complete description of the $[V^{4+}]_A$ centre requires four parameters for the **g** tensor and four parameters for the hyperfine tensor, i.e. the three principal values and one angle for each tensor. The angular dependence in figure 2 requires that one principal axis of each tensor be along either a [100] or a [010] direction, depending on the particular site. Thus, only one angle is needed to specify the directions of the remaining two principal axes in the related (100) or (010) plane. A numerical 'fitting' routine utilizing exact diagonalizations of the 16×16 spin-Hamiltonian matrix provided the final values for the eight parameters. The input data for this fitting process consisted of 235 line positions (i.e. magnetic field values) and their associated microwave frequencies taken at 24 angles uniformly distributed over the three planes in which data were taken. Table 1 contains the final set of parameters for the **g** tensor and the hyperfine tensor for one of the four crystallographically equivalent sites occupied by the $[V^{4+}]_A$ centre.

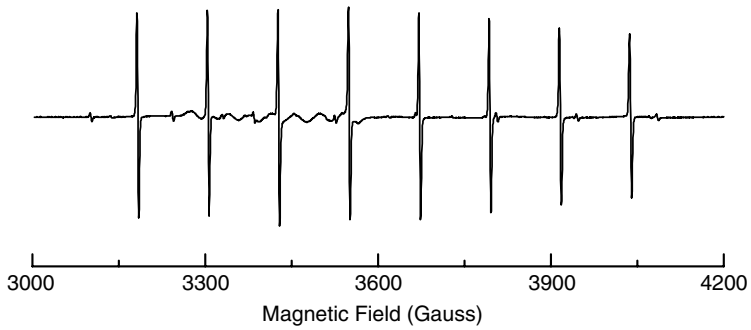

Figure 3. EPR spectrum of the $[V^{4+}]_B$ centre in YVO_4, taken at 30 K with the magnetic field along the [001] direction.

The directions of the principal axes for the remaining three sites are obtained by applying the symmetry elements of the YVO_4 lattice. For simplification, we have used (θ, ϕ) pairs of angles to specify the direction of each principal axis in table 1. The polar angle θ is measured relative to the [001] direction and the azimuthal angle ϕ is measured relative to the [100] direction in the (001) plane with positive rotation from [100] to [010].

3.2. $[V^{4+}]_B$ centre (in as-grown crystals)

The EPR signal referred to as the $[V^{4+}]_B$ centre is shown in figure 3. This spectrum is also present, at varying levels of intensity, in many as-grown YVO_4 crystals. The data in figure 3 were taken at 30 K with the magnetic field parallel to the [001] direction and a 9.443 GHz microwave frequency. Because of a longer spin-lattice relaxation time, the $[V^{4+}]_B$ centre shows microwave-power saturation effects and is best observed between 20 and 50 K. We estimate that the concentration of defects represented by the $[V^{4+}]_B$ spectrum in figure 3 is approximately $9\times10^{16}\,cm^{-3}$. The EPR angular dependence of the $[V^{4+}]_B$ spectrum was recorded in the (010) plane, the $(\bar{1}10)$ plane, and the (001) plane, with data taken at 10° intervals. These results, shown in figure 4 for two planes, are clearly different from the results obtained for the $[V^{4+}]_A$ centre. For an arbitrary direction of magnetic field, there are eight magnetically inequivalent, but crystallographically equivalent, orientations of the defect responsible for the $[V^{4+}]_B$ spectrum. All the eight sites are degenerate when the magnetic field is along the [001] direction, and the EPR spectrum then consists of a single set of eight lines. The eight sites separate into two fourfold degenerate sets if the magnetic field is rotated in the (001) plane from [100] to [010], and two sets of eight lines are observed in the EPR spectra. When the magnetic field is rotated in the (010) plane from [001] to [100] or in the $(\bar{1}10)$ plane from [001] to [110], the eight sites are pairwise degenerate and four sets of eight lines are observed in the EPR spectra.

The spin-Hamiltonian in equation (1) was used to analyse the angular dependence data from the $[V^{4+}]_B$ centre. Because of its lower symmetry, a complete description of the $[V^{4+}]_B$ centre requires six parameters for the **g** tensor and six parameters for the hyperfine tensor. In each case, these six parameters are the three principal values and the three Euler angles (that specify the directions of the principal axes). Numerical fitting using exact diagonalizations provided the best values for these 12 parameters. The input data consisted of 570 line positions and their associated microwave frequencies taken at 28 angles uniformly distributed over the three planes in which data were acquired. The results are given in table 1 for one of the eight crystallographically equivalent sites occupied by the $[V^{4+}]_B$ centre.

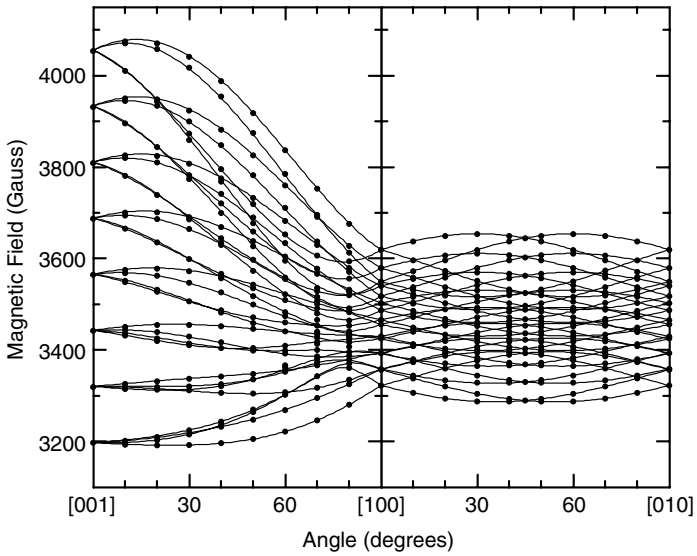

Figure 4. Angular dependence of the $[V^{4+}]_B$ centre for rotations in the (010) and (001) planes. The experimental results, obtained at 30 K, are represented by the discrete data points, while the solid lines were calculated using the **g** and **A** tensors in table 1.

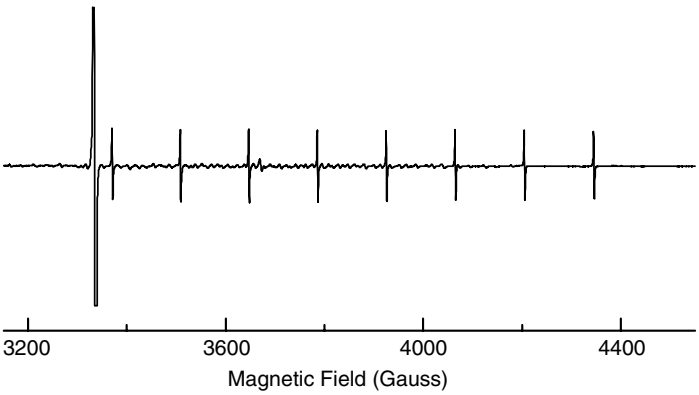

Figure 5. EPR spectrum of the $[V^{4+}]_C$ centre in YVO_4, taken at 15 K with the magnetic field along the [001] direction.

3.3. $[V^{4+}]_C$ centre (in 77 K irradiated crystals)

The EPR signal referred to as the $[V^{4+}]_C$ centre is shown in figure 5. This spectrum was produced during an irradiation with x-rays at 77 K, and the data were taken at 15 K with the magnetic field parallel to the [001] direction and a 9.453 GHz microwave frequency. We estimate that the concentration of defects represented by the $[V^{4+}]_C$ spectrum in figure 5 is approximately $4\times10^{16}\,cm^{-3}$. The additional large EPR line in figure 5 on the low-field side of the $[V^{4+}]_C$ spectrum was also produced by the radiation and is due to the Si^{4+}-h^+ centres initially described by Garces *et al* [22]. We estimate that the concentration of Si^{4+}-h^+ centres in figure 5 is approximately $3\times10^{17}\,cm^{-3}$.

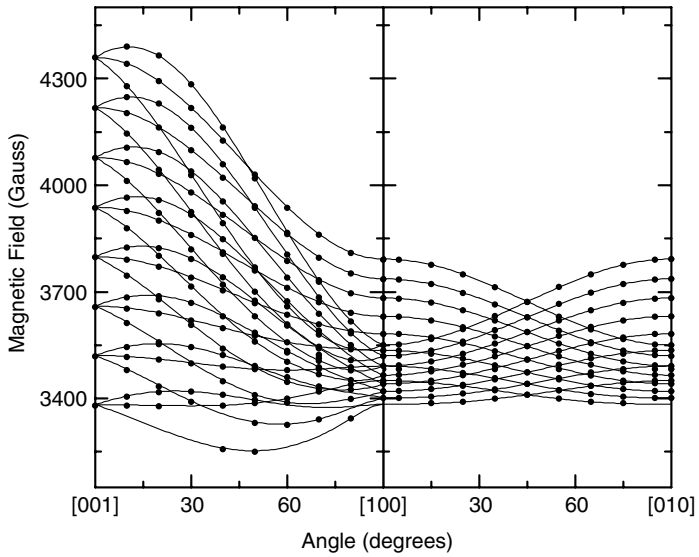

Figure 6. Angular dependence of the $[V^{4+}]_C$ centre for rotations in the (010) and (001) planes. The experimental results, obtained at 15 K, are represented by the discrete data points, while the solid lines were calculated using the **g** and **A** tensors in table 1.

The angular dependence data for the $[V^{4+}]_C$ spectrum was taken at 10° intervals during rotations in the (010) plane the $(\bar{1}10)$ plane and the (001) plane. Results from the (010) and (001) planes are shown in figure 6. The $[V^{4+}]_C$ centre exhibits the same symmetries as the $[V^{4+}]_A$ centre (compare figure 2 to figure 6). For an arbitrary direction of magnetic field, there are four magnetically inequivalent, but crystallographically equivalent, orientations of the defect responsible for the $[V^{4+}]_C$ spectrum. The spectra from these four sites are degenerate when the magnetic field is along the [001] or [110] directions, and one set of eight lines is observed. There are two sets of eight lines when the magnetic field is rotated in the (001) plane or in the $(\bar{1}10)$ plane, and there are three sets of eight lines when the magnetic field is rotated in the (010) plane.

The spin-Hamiltonian in equation (1) was used to analyse the angular dependence data from the $[V^{4+}]_C$ centre. Similar to the $[V^{4+}]_A$ centre, a complete description of the $[V^{4+}]_C$ centre requires four parameters for the **g** tensor and four parameters for the hyperfine tensor. The angular dependence pattern in figure 6 requires that one principal axis of each tensor be along either a [100] or a [010] direction, depending on the particular site. Input data for the fitting process consisted of 284 line positions and their associated microwave frequencies taken at 28 angles uniformly distributed over the three planes where data were acquired. The resulting set of parameters for the **g** tensor and the hyperfine tensor are given in table 1 for one of the four crystallographically equivalent sites occupied by the $[V^{4+}]_C$ centre.

4. Optical absorption results

The relationship between V^{4+} centres and the yellow coloration found in some as-grown YVO_4 crystals was investigated. In figure 7, the absorption band causing the unwanted coloration is shown for five crystals from our set of 14 samples (these five crystals were chosen because they represented a range of absorptions extending from minimal to high). The data in figure 7

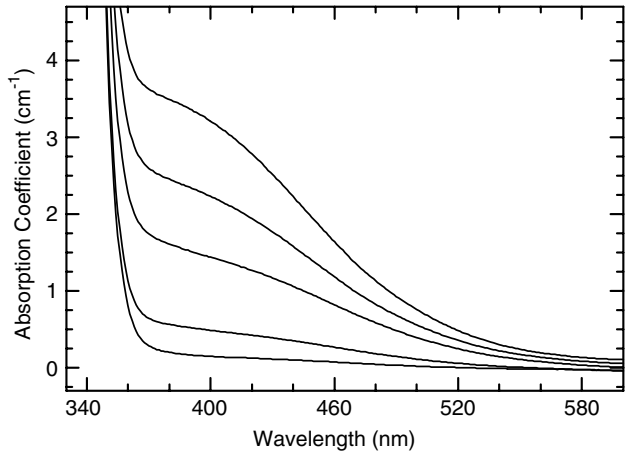

Figure 7. Optical absorption from five YVO_4 crystals showing the possible variation in intensity of the broad near-edge band responsible for the yellow coloration.

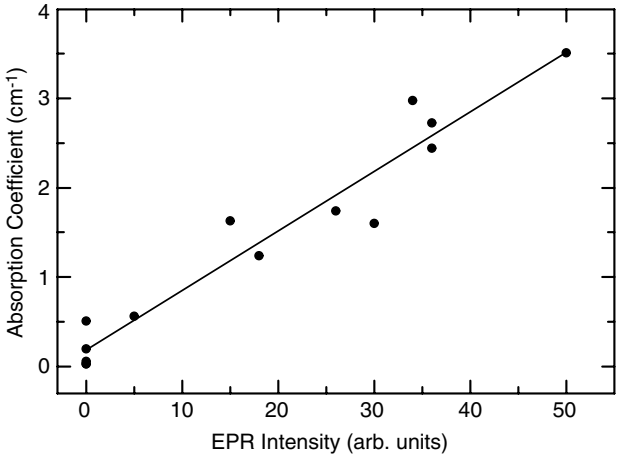

Figure 8. Plot of the intensity of the optical absorption band (measured at 380 nm) versus the intensity of the EPR signal from the $[V^{4+}]_A$ centre in a set of 14 undoped YVO_4 crystals. Several of the data points overlap.

were taken at room temperature with unpolarized light propagating along the [100] axis of the samples (the optical path length for each sample was 8.2 mm). The absorption band responsible for the yellow coloration is not well resolved. It appears simply as a broad shoulder extending below the band edge (from 350 nm to approximately 550 nm).

Both the $[V^{4+}]_A$ and $[V^{4+}]_B$ centres are present in the as-grown crystals and thus are candidates for the defect causing the yellow coloration. In a search for possible correlations, the intensities of the EPR signals from these two centres were compared with the intensity of the absorption band (measured at 380 nm) causing the yellow coloration in our set of 14 undoped YVO_4 crystals. We found a good correlation of the absorption intensity with the $[V^{4+}]_A$ centre, and no correlation with the $[V^{4+}]_B$ centre. Figure 8 shows the EPR intensity of the $[V^{4+}]_A$ centre plotted versus the intensity of the near-edge absorption band for the 14

samples. The $[V^{4+}]_C$ centres are not present in the as-grown crystals, and thus cannot be responsible for the yellow coloration.

5. Discussion

A primary goal of our present investigation is to suggest the most likely models for the three centres causing the $[V^{4+}]_A$, $[V^{4+}]_B$, and $[V^{4+}]_C$ EPR signals in undoped YVO_4 crystals. We start with a review of the major point defects in this material. The two dominant unintentional impurities nearly always present in YVO_4 crystals grown by the Czochralski technique are silicon and zirconium. Our glow discharge mass spectrometry (GDMS) results show that their concentrations usually fall within the range of $2–8\times10^{17}\,cm^{-3}$ for silicon and $0.9–2\times10^{17}\,cm^{-3}$ for zirconium. The silicon enters the lattice as Si^{4+} ions and substitutes for V^{5+} ions while the zirconium enters the lattice as Zr^{4+} ions and substitutes for Y^{3+} ions. Thus, they provide charge compensation for each other in the as-grown crystal. The ionic radii of these impurities are important factors in determining which site each ion occupies (e.g. 0.26 Å for four-coordinated Si^{4+} and 0.355 Å for four-coordinated V^{5+}, compared with 0.84 Å for eight-coordinated Zr^{4+} and 1.02 Å for eight-coordinated Y^{3+}). Intrinsic defects that also provide charge compensation for Si^{4+} ions in YVO_4 are oxygen vacancies trapping one electron and vanadium ions (V^{4+}) replacing yttrium ions (Y^{3+}), i.e. vanadium antisites. These latter two defects represent only small deviations from stoichiometry in most YVO_4 crystals. Thus far, there are no available optical or EPR results to suggest that ions other than hydrogen [25] can exist at interstitial sites in YVO_4 crystals, or that cation vacancies occur in significant concentrations.

We have observed with EPR that Si^{4+}-h^+ centres [22] are present in some of our as-grown YVO_4 crystals (i.e. before any irradiation). This suggests that the concentration of Si^{4+} ions in these particular crystals exceeds the combined concentrations of the defects providing the needed charge compensation. Without sufficient charge compensators, these crystals achieve charge neutrality by forming holes (i.e. missing electrons), which then become trapped on an oxygen ion adjacent to a Si^{4+} ion. If the number of silicon impurities is approximately constant, the concentration of Si^{4+}-h^+ centres will be greatest in those crystals having the smallest concentrations of charge compensators. Seven out of the 14 samples in our set had Si^{4+}-h^+ centres present in their as-grown state, and a very clear anti-correlation was found between the intensity of the optical absorption at 380 nm and the intensity of the EPR signal representing the Si^{4+}-h^+ centres. In other words, the largest Si^{4+}-h^+ centre EPR signal is observed in the YVO_4 sample with the smallest absorption near the band edge. We interpret this Si^{4+}-h^+ result to mean that at least one of the Si^{4+} charge compensators makes a significant contribution to the observed yellow coloration.

Two of the centres providing charge compensation for Si^{4+} ions are expected to be paramagnetic in as-grown YVO_4 crystals. A V^{4+} ion adjacent to an oxygen vacancy has one unpaired electron, and charge compensates one Si^{4+} ion replacing a V^{5+} ion in the lattice. A V^{4+} ion substituting for a Y^{3+} ion also has one unpaired electron, and charge compensates one Si^{4+} ion in the lattice. In our present study, the $[V^{4+}]_A$ and $[V^{4+}]_B$ centres observed in the as-grown crystals are candidates for these paramagnetic charge compensators. A distinguishing feature of these two EPR signals is the maximum number of magnetically inequivalent, but crystallographically equivalent, sites for each centre (four for the $[V^{4+}]_A$ centre and eight for the $[V^{4+}]_B$ centre). This difference in defect symmetry leads us to suggest that the $[V^{4+}]_A$ centre is a V^{4+} ion adjacent to an oxygen vacancy and the $[V^{4+}]_B$ centre is a V^{4+} ion substituting off-centre for a Y^{3+} ion. One of the principal axes (see table 1) for each of the four equivalent sites for the $[V^{4+}]_A$ centre is along either a [100] or [010] direction. This is consistent with a

model in which the V^{4+} ion is located adjacent to an oxygen vacancy. In contrast, the $[V^{4+}]_B$ centre has lower symmetry (eight distinguishable sites) and none of its principal axes are along high-symmetry directions in the lattice. This latter behaviour is consistent with a V^{4+} ion sitting off-centre at a Y^{3+} site. Because of its smaller size, the V^{4+} ion could easily move off the centre of the Y^{3+} site (compare the 0.72 Å ionic radius of eight-coordinated V^{4+} with the 1.02 Å ionic radius of eight-coordinated Y^{3+}).

The $[V^{4+}]_C$ centres are formed in YVO_4 during an exposure to ionizing radiation at 77 K. Simultaneous formation of Si^{4+}-h^+ centres during the irradiation indicates that the $[V^{4+}]_C$ centres became paramagnetic by trapping an electron. However, these trapped electrons have only limited thermal stability. The $[V^{4+}]_C$ centres are destroyed when the crystal is raised to room temperature (this thermal destruction of the $[V^{4+}]_C$ centres must occur when these centres release their trapped electrons, since the Si^{4+}-h^+ centres are known to be stable above room temperature). We suggest that the $[V^{4+}]_C$ centre is a V^{4+} ion at a regular vanadium site with a nearby Zr^{4+} ion on a Y^{3+} site providing stability. In visualizing this defect, consider a nearest-neighbour pair of Zr^{4+} and V^{5+} ions located on substitutional sites along the *c*-axis of the crystal. To achieve the minimum energy for the $[V^{4+}]_C$ centre, the electron is trapped on an adjacent V^{5+} ion, thus forming a V^{4+} ion, instead of being trapped directly on the Zr^{4+} ion to form a Zr^{3+} ion. The Zr^{4+} ion provides only a small stabilizing effect and the V^{4+} ion cannot 'hold' the extra electron at room temperature. We note that none of the principal axes of the $[V^{4+}]_C$ centre are aligned exactly along the *c*-axis. The lower symmetry observed for this centre (i.e. its four crystallographically equivalent orientations) is most likely a result of the Zr^{4+} ion moving slightly off the centre of the normal Y^{3+} position, in either a (100) or (010) plane. This off-centre movement would be expected because of the smaller size of the Zr^{4+} ion, relative to the Y^{3+} ion.

In addition to the three EPR spectra reported in section 3, we have observed a fourth very broad spectrum at 10 K in as-grown samples that have significant yellow coloration. When the magnetic field is parallel to the *c*-axis of the crystal, this spectrum is centred approximately on $g = 1.74$ and consists of eight barely resolved lines with an average splitting near 200 G. The spectrum is difficult to observe, even though it represents a large concentration of defects, approaching $1\times10^{19}\,cm^{-3}$ or more in these crystals, and an angular dependence could not be obtained. As-grown crystals with little or no yellow coloration did not show this spectrum. Also, there were no measurable changes in this spectrum as a result of exposure to ionizing radiation. Although insufficient data exist to establish a model for this fourth EPR spectrum, we suggest that it may represent V^{3+} (d^2) ions next to oxygen vacancies. These $S = 1$ centres are electrically neutral, relative to the regular lattice, and do not require charge compensation. They presumably are formed when an oxygen atom leaves the crystal during growth or, equivalently, when a doubly ionized oxygen vacancy traps two electrons. Although each oxygen ion has one vanadium neighbour and two yttrium neighbours located within a (100) or (010) plane, both of the trapped electrons will be localized on the vanadium ion as a result of its larger electron affinity. Because of the presence of the oxygen vacancy, we expect that the V^{3+} ions will experience a large electric crystal field [26] and the only observable EPR transition at 9.45 GHz will then be $\Delta M_S = \pm2$. At higher microwave frequencies, the normal doublet associated with an $S = 1$ spin system (i.e. the $\Delta M_S = \pm1$ transitions) may be observed.

6. Summary

We have used EPR to characterize three V^{4+} centres in a set of 14 Czochralski-grown YVO_4 crystals. The models suggested for these centres are a V^{4+} ion adjacent to an oxygen vacancy, a

V^{4+} ion replacing a Y^{3+} ion, and a V^{4+} ion near a Zr^{4+} impurity ion on a Y^{3+} site. The first two centres are present in as-grown crystals, while the third centre is only present after exposure to ionizing radiation at low temperature. A correlation was found between the number of V^{4+} ions adjacent to oxygen vacancies and the intensity of the optical absorption band that gives YVO_4 crystals an yellow appearance. The role played by Si^{4+} impurity ions and their related charge compensators is described, and the possible observation of V^{3+} ions ($S = 1$ centres) adjacent to oxygen vacancies is discussed.

Acknowledgment

The work at West Virginia University was supported by Northrop Grumman Space Technology (Synoptics).

References

[1] Wu S, Wang G, Xie J, Wu X and Li G 2003 *J. Crystal Growth* **249** 176
[2] Ryba-Romanowski W 2003 *Crystal Res. Technol.* **38** 225
[3] Zdobnikov A Y, Kislovskii L D and Korovkin A M 1987 *Opt. Spectrosc.* **62** 620
[4] Cui C, Zhang Y, Zhuang X, Tang D and Mao H 1999 *Chinese J. Lasers* A **26** 145
[5] Shi H, Zhang G and Shen H 2001 *J. Synth. Crystals* **30** 85
[6] DeShazer L G 2002 *SPIE Proc.* **4481** 10
[7] Xiang Q and Huang D 1996 *Chinese J. Lasers* A **23** 225
[8] Fan X, Rong C T, Fainman Y and Ford J F 1996 *Opt. Lett.* **21** 516
[9] Damask J N, Myers P R, Boschi A and Simer G J 2003 *IEEE Photon. Technol. Lett.* **15** 1612
[10] Waichman K and Kalisky Y 2002 *Opt. Mater.* **19** 149
[11] Du K, Li D, Zhang H, Shi P, Wei X and Diart R 2003 *Opt. Lett.* **28** 87
[12] Garcia-Lopez J H, Aboites V, Kir'yanov A, Damzen M J and Minassian A 2003 *Opt. Commun.* **218** 155
[13] Liu J, Yang J and He J 2003 *Opt. Laser Technol.* **35** 431
[14] Zhang H, Chao M, Gao M, Zhang L and Yao J 2003 *Opt. Laser Technol.* **35** 445
[15] Koechner W 1999 *Solid-State Laser Engineering* 5th edn (Berlin: Springer) pp 63–5
[16] Chen F, Wang X, Li S, Fu G, Wang K, Lu Q, Shen D, Nie R and Ma H 2003 *J. Appl. Phys.* **94** 4708
[17] Spaeth J M, Niklas J R and Bartram R H 1992 *Structural Analysis of Point Defects in Solids* (Berlin: Springer)
[18] Ranon U 1968 *Phys. Lett.* A **28** 228
[19] Rosenthal J, Riley R F and Ranon U 1969 *Phys. Rev.* **177** 625
[20] Guillot-Noel O, Simons D and Gourier D 1999 *J. Phys. Chem. Solids* **60** 555
[21] Misra S K, Isber S, Capobianco J A and Cavalli E 1999 *Chem. Phys.* **240** 313
[22] Garces N Y, Halliburton L E, Stevens K T, Shone M and Foundos G K 2002 *J. Appl. Phys.* **91** 1354
[23] Jablonski R, Kaczmarek S M, Swirkowicz M and Lukasiewicz T 2000 *J. Alloys Compounds* **300–301** 310
[24] Chakoumakos B C, Abraham M M and Boatner L A 1994 *J. Solid State Chem.* **109** 197
[25] Kovacs L, Erdei S and Capelletti R 1999 *Sol. State Commun.* **111** 95
[26] Lambe J and Kikuchi C 1960 *Phys. Rev.* **118** 71